Genomics & Informatics Vol. 7(2) 97-106, June 2009

High-concentration Epigallocatechin Gallate Treatment Causes Endoplasmic Reticulum Stress-mediated Cell Death in HepG2 Cells

Joon-Ik Ahn, Kyoung Ji Jeong, Moon-Jeong Ko, Hee Jung Shin, Hye Joo Chung* and Ho-Sang Jeong*

Molecular Pharmacology Division, Pharmacological Research Department, National Institute of Toxicological Research, Seoul 122-704, Korea

Abstract

Epigallocatechin gallate (EGCG), a well-known antioxidant molecule, has been reported to cause hepatotoxicity when used in excess. However, the mechanism underlying EGCG-induced hepatotoxicity is still unclear. To better understand the mode of action of EGCG-induced hepatotoxicity, we examined the effect of EGCG on human hepatic gene expression in HepG2 cells using microarrays. Analyses of microarray data revealed more than 1300 differentially expressed genes with a variety of biological processes. Upregulated genes showed a primary involvement with protein-related biological processes, such as protein synthesis, protein modification, and protein trafficking, while downregulated genes demonstrated a strong association with lipid transport. Genes involved in cellular stress responses were highly upregulated by EGCG treatment, in particular genes involved in endoplasmic reticulum (ER) stress, such as GADD153, GADD34, and ATF3. In addition, changes in genes responsible for cholesterol synthesis and lipid transport were also observed, which explains the high accumulation of EGCG-induced lipids. We also identified other regulatory genes that might aid in clarifying the molecular mechanism underlying EGCG-induced hepatotoxicity.

Keywords: endoplasmic reticulum stress, epigallocatechin gallate, hepatotoxicity, microarray

Introduction

Green tea is a traditional Asian beverage made from the leaves of *Camellia sinensis* and contains several polyphenolic components, such as catechin, epicatechin, epicatechin gallate (ECG), epigallocatechin (EGC), and epigallocatechin gallate (EGCG).

In addition to its prominent role as a common beverage, green tea has demonstrated profound biochemical and pharmacological activities, including antioxidative activities and anti-inflammatory and anticarcinogenic properties (Isbrucker *et al*., 2006). The beneficial effects of green tea on health have been backed by multiple scientific reports, which have proposed the involvement of green tea in various biological processes, such as inhibition of: telomerase, mitogen-activated protein kinase (MAPK), activator protein-1, nuclear factor (NF)-kB, binding of epidermal growth factor to its receptor, angiogenesis, and activation of apoptosis (Vittal *et al*., 2004).

However, it is becoming more apparent that green tea compounds might also cause deleterious effects at pharmacological concentrations in certain cases (Lambert *et al*., 2007). For example, in France and Spain, cases of hepatic attack have been reported after the use of hydroalcoholic extracts of green tea as a complement of diets. These observations have led to the suspension of marketing authorization of these products in both countries. In animal models, EGCG causes a high mortality rate in adult female Swiss Webster mice and hepatotoxicity in immature C57BL/6 female mice (Galati *et al*., 2006; Goodin and Rosengren, 2003). Additionally, recent studies have shown that several phenolic antioxidant food additives can accelerate oxidative damage to DNA, proteins, and carbohydrates, despite their antioxidative action. The molecular mechanism of prooxidative action and hepatotoxicity that are induced by EGCG remains poorly understood. Galati *et al*. (2006) reported that cell death induced by EGCG was associated with increased production of reactive oxygen species (ROS) and depletion of reduced glutathione (GSH) and catechol-o-methyltransferase (COMT). The mechanism of EGCG-induced cell death was suggested in previous reports, which implicated the apoptosis pathway (Schmidt *et al*. 2005) and the endoplasmic reticulum (ER) stress-related pathway (Dodo *et al*., 2008).

To gain insight into the molecular mechanism underlying EGCG-induced cytotoxicity, we used a microarray approach, which allowed us to observe the global effects of EGCG on hepatic gene expression. Time course

*Corresponding author: E-mail hosa33@kfda.go.kr
hjchung@kfda.go.kr
Tel +82-2-380-1804, Fax +82-2-388-6457
Accepted 4 June 2009

observations of the gene expression profile were made. We propose in the present study that hepatic cell death resulting from high-concentration EGCG treatment is mainly caused by ER stress.

Methods

Chemicals

EGCG was purchased from Sigma (St. Louis, MO, USA). DMEM, fetal bovine serum (FBS), penicillin/streptomycin, TRIzol, and DEPC-treated water were obtained from Invitrogen (Carlsbad, CA, USA).

Cell culture

The HepG2 cell line was cultured in DMEM medium supplemented with 10% heat-inactivated FBS, 100 U/ml penicillin, and 100 mg/ml streptomycin and maintained in a monolayer culture at 37°C in an incubator of humidified air with 5% CO_2. Subconfluent cells (80%) were passaged with a solution containing 0.05% trypsin and 0.02% EDTA.

Cell viability assay

HepG2 cells were treated with test substances dissolved in 10% DMSO for 24 h. After the treatment, cell viability was assessed using the resazurin assay (CellTiter Blue®, Promega, Madison, WI, USA). Cells were incubated with medium containing resazurin. A kinetic assay of resorufin, produced from resazurin by vital cells, was performed by measuring its absorbance (570 nm) in a SpectraMax microplate reader (Molecular Devices, Sunnyvale, CA, USA). The absorbance at 600 nm was used as reference.

RNA isolation and DNA microarray

Total RNA was extracted using Trizol at each time point in accordance with the manufacturer's procedures. RNA quantification and purity (260/280 ratio) were determined with a UV/VIS spectrophotometer (ND-1000, NanoDrop Technologies, Wilmington, DE, USA).

The Applied Biosystems Human Genome Survey Arrays (Applied Biosystems, Foster City, CA, USA), which contain 60-mer oligonucleotide probes representing a set of 32,878 individual mouse genes and more than 250 control probes, were used for differential gene expression profiles. Microarray experiments were performed according to the manufacturer's instructions. Digoxigenin (DIG)-UTP-labeled cRNA was generated from 5 μg of total RNA and amplified using a chemiluminescent reverse transcription (RT) in vitro transcription labeling kit (Applied Biosystems). Briefly, each microarray was prehybridized in hybridization buffer with blocking reagent at 55°C for 1 h. DIG-labeled cRNA targets (10 μg) were fragmented to 100?400 bp and hybridized with each prehybridized microarray at 55°C for 16 h. The arrays were washed with hybridization wash buffer and then with chemiluminescence rinse buffer. Chemiluminescent signals were generated by incubating the arrays with anti-DIG-alkaline phosphatase and chemiluminescence substrate. Images were collected for each microarray using the 1700 Chemiluminescent Microarray Analyzer (Applied Biosystems). Microarray images were autogridded, and the chemiluminescent signals were quantified, corrected for background, spatially normalized, and exported for a quality report. Microarray data with quality reports above the manufacturer's threshold were used for further analysis.

Analysis of microarray expression data

Signal intensities were imported into GenPlex software (Istech Inc, Korea), where interarray quantile normalization was performed in order to minimize the effect of external variables introduced into the data. Quality filtering of unreliable spots (flag value $<$ 100 and S/N $<$ 3) was performed before normalization. Then, the expression intensities were log2-transformed. Differentially expressed genes (DEGs) were selected by one-way ANOVA, and correction for multiple testing was then performed using Benjamini-Hochberg multiple testing to derive a false discovery rate estimate from the raw p-values. A false discovery rate of 1% was used as a cutoff for statistical significance. We took the average value from the gene expression ratio obtained in 3 or more biological replicates.

For further analysis, DEGs were divided into gene clusters according to expression level at each time point. Hierarchical clustering was applied to genes using Euclidean distance as a similarity measurement, as implemented in the Genesis software program (http://genome.tugraz.at). Additionally, DEGs were divided into categories according to biological process using the PANTHER (Protein ANalysis THrough Evolutionary Relationships) Protein Classification System (Applied Biosystems, https://panther.appliedbiosystems.com).

Semiquantitative and real-time quantitative RT-PCR

For semiquantitative and real-time quantitative RT-PCR, glyceraldehydes-3-phosphate dehydrogenase (GAPDH) was used as an internal control with the 5'- ccatcatgaagtgtgacgttg -3' and 5'- gtgctaggagccagagcagta -3'

primer set. For each sample, the same total RNA used for microarray hybridization was reverse-transcribed using 1 μM oligo (dT) primer with Superscript Ⅲ reverse transcriptase (Invitrogen). The thermal profiles consisted of 94°C for 5 min for initial denaturing, followed by 25～35 cycles of 94°C for 30 s, 55～65°C for 30 s, and 72°C for 30 s to 1 min. All RT-PCR reactions were repeated at least 3 times. Triplicate real-time RT-PCR experiments were performed using the MiniOpticon system (Bio-Rad, Hercules, CA) and the DyNAmo Flash SYBR Green qPCR kit (Finnzymes, Espoo, Finland). A melting curve was obtained for each PCR product after each run to confirm that the signal corresponded to a unique amplicon of the product size. The primers were 5'- gaa gtg agt gct tct gcc atc -3' and 5'- act ttc cag ctt ctc cga ctc-3' for activating transcription factor 3 (ATF3); 5'- ttt cca gac tga tcc aac tgc -3' and 5'- acc act ctg ttt ccg ttt cct g -3' for DNA damage-inducible transcript 3 (DDIT3/GADD153/CHOP); 5'- gat gaa gag gag ggt gag gtc -3' and 5'- aca cct gta gca gga gtg gaa g -3' for protein phosphatase, regulatory subunit 15A (PPP1R15A/GADD34); 5'- cca tac gga gaa acc aga aca -3' and 5'- ggt ggc ctt cgt act tct ctt g -3' for seven in absentia homolog 2 (SIAH2); 5'- gct ggt acc cag ctc ctc tac -3' and 5'- gtt ctc cag cac cag ctt ctt c -3' for tribbles homolog 3 (TRIB3); 5'- tca gtc acg ggt gag cag tat g -3' and 5'- caa agt ctc tgc caa gag tgg -3' for stromal cell-derived factor 2-like 1 (SDF2L1); 5'- cct tgt tcc aga gca gat gtc -3' and 5'- att cca cca aaa act gca cac -3' for choroideremia-like (CHML); and 5'- tca gct ttt tcc aga gat cca g -3' and 5'- cta tcc tgt cga ctt gct tgg -3' for YKT6 v-SNARE homolog (YKT6).

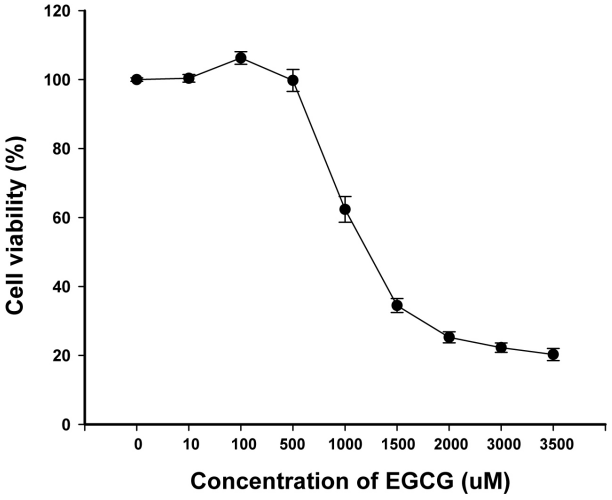

Fig. 1. Resazurin assay results from HepG2 cells treated with EGCG. Cells were incubated with the indicated concentrations of EGCG for 24 hr, followed by Resazurin assay. Each concentration was assayed in triplicate within an experiment. Data are expressed as percentage of untreated cells, and error bars represent the standard error of the mean.

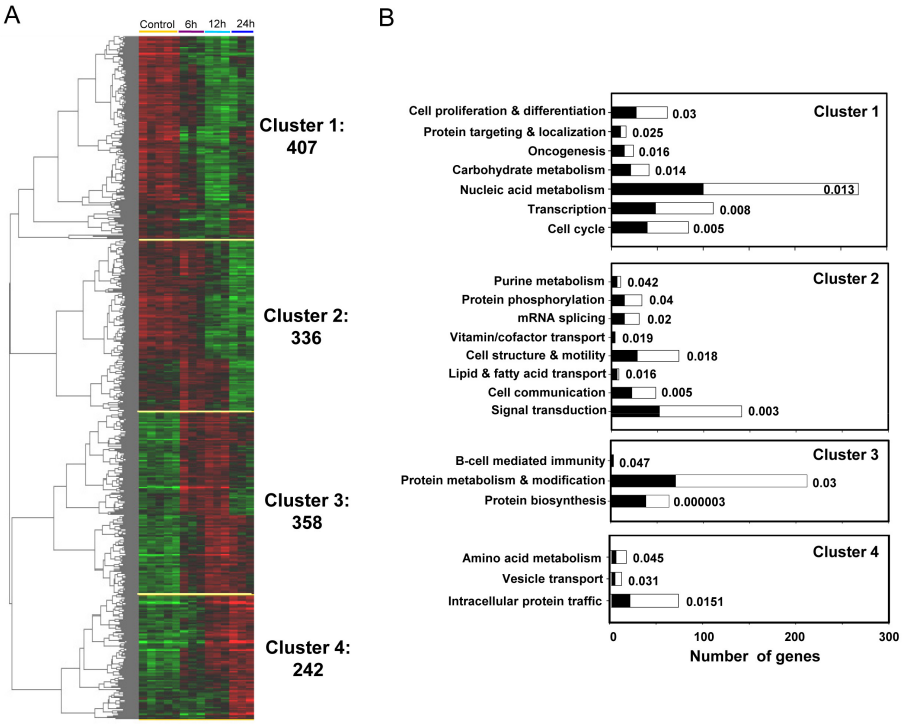

Fig. 2. (A) Hierarchical clustering of 1343 genes that showed differential expression patterns. The genes were clustered by Euclidean distance; 1343 genes were classified into 4 clusters. The intensity of red and green is proportional to the relative gene induction (red) or repression (green). (B) Primary biological processes for each cluster. The PANTHER gene expression data analysis tool was used to identify significantly overrepresented biological processes for each cluster. The bar graph indicates the numbers of genes belonging to specific biological processes. The p value for each biological process is indicated.

Statistical analysis

All experiments were carried out 3 times. Results are presented as mean values±SE.

Results

Cell viability following treatment with EGCG

The effect of EGCG on HepG2 viability was monitored by resazurin assay, which measures the reducing capacity of mitochondria in cells. Based on the cell viability assay results, it seemed that the treatment of EGCG at low concentrations (10-100 uM) increased the viability of the cells but not at higher concentrations (1000-3500 uM). At higher concentrations, rather, EGCG caused a significant decrease in cell viability (Fig. 1). The lethal concentration 30 (LC_{30}) of EGCG against HepG2 cells was determined as 850 uM, according to nonlinear regression analysis. EGCC at 850 uM was used for the following experiments.

Identification of differentially expressed genes

Gene expression profiling was performed to examine the temporal changes of gene expression in EGCG-treated HepG2 cells. Total RNA was prepared from the cells treated with 850 uM of EGCG for 6, 12, 24 h, and 0 h

Table 1. Protein biosynthesis- and protein metabolism/modification-related genes regulated by EGCG

Probe id	Gene symbol	Gene name	6h ratio -log2	12h ratio -log2	24h ratio -log2
Protein biosynthesis					
120032	EIF2C2	eukaryotic translation initiation factor 2C, 2	0.897	0.778	0.831
203208	EIF3S12	eukaryotic translation initiation factor 3, subunit 12	0.604	0.826	0.394
185066	ITGB4BP	integrin beta 4 binding protein	1.210	1.495	0.733
124345	LOC134505	similar to eukaryotic translation initiation factor 3 subunit k	0.851	1.265	0.508
132913	MRPL17	mitochondrial ribosomal protein L17	0.773	0.977	0.394
165531	MRPL21	mitochondrial ribosomal protein L21	0.781	1.310	0.601
105643	MRPL40	mitochondrial ribosomal protein L40	0.653	0.722	0.700
149811	MRPL49	mitochondrial ribosomal protein L49	0.580	1.299	0.973
167428	RPL28	ribosomal protein L28	0.769	0.979	0.757
184007	RPS19	ribosomal protein S19	0.379	1.038	0.739
141447	RPS9	ribosomal protein S9	0.579	1.134	0.862
Protein metabolism & modification					
208619	BAG4	BCL2-associated athanogene 4	1.697	1.673	1.389
171701	DNAJB6	DnaJ (Hsp40) homolog, subfamily B, member 6	1.317	1.326	0.356
140616	DUSP23	dual specificity phosphatase 23	0.982	1.245	0.550
121612	DUSP5	dual specificity phosphatase 5	2.526	1.996	0.794
151197	F12	coagulation factor XII (Hageman factor)	0.830	1.115	0.971
165933	FLJ22405	hypothetical protein FLJ22405	0.997	0.958	0.277
111748	HTRA1	HtrA serine peptidase 1	0.724	0.854	-0.460
131931	ICAM3	intercellular adhesion molecule 3	1.046	1.715	1.360
163269	IMMP2L	IMP2 inner mitochondrial membrane peptidase-like (S. cerevisiae)	0.887	1.461	0.380
147822	LATS2	LATS, large tumor suppressor, homolog 2 (Drosophila)	0.882	1.758	0.177
135861	MGC11102	hypothetical protein MGC11102	0.793	1.643	1.231
182792	MSI2	musashi homolog 2 (Drosophila)	1.161	1.857	1.196
165933	MTMR14	myotubularin related protein 14	0.997	0.958	0.277
204476	PPIH	peptidylprolyl isomerase H (cyclophilin H)	0.822	0.632	0.224
184060	PPP2R4	protein phosphatase 2A, regulatory subunit B' (PR 53)	0.711	0.859	0.451
139782	PRSS21	protease, serine, 21 (testisin)	0.897	0.758	-0.091
135806	RNF113A	ring finger protein 113A	1.069	1.250	0.691
163408	SIAH2	seven in absentia homolog 2 (Drosophila)	2.187	2.766	1.249
151579	ST3GAL1	ST3 beta-galactoside alpha-2,3-sialyltransferase 1	0.609	0.769	-0.749
113737	TRIB3	tribbles homolog 3 (Drosophila)	1.597	2.620	2.246
197340	UBC	ubiquitin C	0.768	0.925	0.321
186200	UBE2L3	ubiquitin-conjugating enzyme E2L 3	0.722	0.843	0.399
197127	WARS	tryptophanyl-tRNA synthetase	0.918	1.291	1.331

†Unknown genes removed.

(the control). The cRNAs were subsequently synthesized and hybridized. Analyses revealed that EGCG treatment significantly ($p < 0.01$) altered the expression of 1343 genes (http://kotis.nifds.go.kr). Interestingly, activating transcription factor 3 (ATF3) and N-myc downstream-regulated gene 1 (NDRG1) showed marked overexpression (more than 5-fold), while inhibitor of DNA binding 1 (ID1) revealed a drastic downregulation (more than 10-fold) by EGCG treatment at all 3 time points.

Clustering and functional enrichment analysis

To characterize patterns of transcript expression during the time course, hierarchical clustering was performed on the 1343 genes, and these genes were classified into 4 clusters (Fig. 2A). The temporal cluster analysis revealed 4 clusters of transcripts that were either downregulated (cluster 1; 407 genes and cluster 2; 336 genes) or upregulated (cluster 3; 358 genes and cluster 4; 242 genes). Genes in cluster 1 showed a trend of expression that decreased up to 12 h and increased slightly at 24 h. Genes in cluster 2 showed a gradual decrease up to 24 h. On the contrary, genes in cluster 3 showed overexpression up to 12 h and slight underexpression at 24 h. Cluster 4 contained genes with gradually increasing expression up to 24 h.

To understand the effect of EGCG treatment on HepG2 cells, overrepresented biological processes of each cluster were identified using the PANTHER gene expression data analysis tool (Fig. 2B). According to the analyses, biological processes, such as cell cycle, transcription, nucleic acid metabolism, carbohydrate metabolism, oncogenesis, protein targeting/localization, and cell proliferation/differentiation, showed significant enrichment in cluster 1, and signal transduction, cell communication, lipid/fatty acid transport, cell structure and motility, vitamin/cofactor transport, mRNA splicing, protein phosphorylation, and purine metabolism were in cluster 2.

Clusters 3 and 4 also revealed enrichment of certain biological processes, such as protein biosynthesis, protein metabolism and modification, and B cell immunity for cluster 3 and intracellular protein traffic, vesicle transport, and amino acid metabolism for cluster 4.

EGCG increases expression of genes related to protein biosynthesis and protein metabolism/modification

Treatment with EGCG led to elevated expression of genes associated with protein biosynthesis and protein modification (Table 1), including eukaryotic translation

Table 2. Intracellular protein traffic-related genes regulated by EGCG

Probe id	Gene symbol	Gene name	6h ratio -log2	12h ratio -log2	24h ratio -log2
Intracellular protein traffic					
115761	ARL1	ADP-ribosylation factor-like 1	0.417	1.044	1.263
217838	CHML	choroideremia-like (Rab escort protein 2)	1.105	1.738	2.416
166994	CHMP5	chromatin modifying protein 5	−0.001	0.433	0.887
147300	CSNK1G3	casein kinase 1, gamma 3	−0.187	0.129	0.956
171123	EXOC2	exocyst complex component 2	0.297	−0.031	0.969
159351	KDELR2	KDEL endoplasmic reticulum protein retention receptor 2	0.110	0.639	1.008
157883	NAPG	N-ethylmaleimide-sensitive factor attachment protein, gamma	0.781	1.421	2.015
221608	NUP107	nucleoporin 107kDa	−0.159	1.404	1.182
114948	NUP50	nucleoporin 50kDa	0.663	1.031	1.202
123733	PPIL3	peptidylprolyl isomerase (cyclophilin)-like 3	0.206	0.427	1.348
156761	RAB18	RAB18, member RAS oncogene family	−0.068	0.419	0.736
112058	RAB8B	RAB8B, member RAS oncogene family	0.980	1.329	1.549
197182	RER1	RER1 retention in endoplasmic reticulum 1 homolog (S. cerevisiae)	−0.135	1.013	1.135
155479	RTN3	reticulon 3	0.385	0.470	1.470
181273	SAR1A	SAR1 gene homolog A (S. cerevisiae)	1.004	1.880	1.965
171123	SEC5L1	SEC5-like 1 (S. cerevisiae)	0.297	−0.031	0.969
169954	SNX6	sorting nexin 6	0.424	0.290	0.615
209483	TMED7	transmembrane emp24 protein transport domain containing 7	0.779	1.297	1.787
121895	TOM1L1	target of myb1-like 1 (chicken)	−0.043	0.758	1.459
122318	TRAM1	translocation associated membrane protein 1	−0.010	0.824	1.479
209190	WDR24	WD repeat domain 24	0.254	2.244	4.139
117439	YIPF4	Yip1 domain family, member 4	0.526	1.308	1.222
163460	YKT6	SNARE protein Ykt6	0.859	1.436	1.625

initiation factors (EIFs), mitochondrial ribosomal proteins (MRPLs), ribosomal proteins (RPLs), dual specificity phosphatases (DUSPs), peptidylprolyl isomerase H (PPIH), protein phosphatase 2A, regulatory subunit B(PPP2R4), and protease, serine, 21(PRSS21). Many of these transcripts showed significant elevation in expression (more than 2-fold) at 12 h.

Effects of EGCG on intracellular protein traffic-related genes

Many genes related to protein trafficking were upregulated by EGCG treatment (Table 2). Transcripts in this biological process showed a peculiar increase in expression at 24 h. In particular, genes like choroideremia-like (CHML), N-ethylmaleimide-sensitive factor attachment protein gamma (NAPG), and WD repeat domain 24 (WDR24) showed overexpression, greater than 4-fold, at 24 h.

EGCG alters expression of several genes related to lipid metabolism

EGCG treatment turned out to cause underexpression of many genes related to lipid metabolism (Table 3). The expression of genes involved in lipid transport, including caveolin 1 (CAV1), niemann-pick disease, type C1 (NPC1), oxysterol-binding protein-like 1A (OSBPL1A), and clusterin (CLU), were downregulated, as shown by PANTHER gene expression data analysis (Table 1). In particular, NPC1 has been reported to be involved in the intracellular trafficking of cholesterol (Pacheco and Lieberman, 2008). On the other hand, the expression of genes related to the cholesterol biosynthetic pathway, including isopentenyl-diphosphate delta isomerase 1 (IDI1), farnesyl-diphosphate farnesyltransferase 1 (FDFT1), 3-hydroxy-3-methylglutaryl-coenzymeA reductase (HMGCR), and HMG-coenzyme A synthase 1 (HMGCS1), was upregulated at 24 h after EGCG treatment. These observations indicate that treatment with EGCG induces the synthesis and accumulation of cholesterol in HepG2 cells.

Table 3. Lipid metabolism-related genes regulated by EGCG

Probe id	Gene symbol	Gene name	6h ratio -log2	12h ratio -log2	24h ratio -log2
185568	PLA2G4A	phospholipase A2, group IVA (cytosolic, calcium-dependent)	−0.848	-2.224	−2.178
158523	PAFAH1B1	platelet-activating factor acetylhydrolase, isoform Ib, alpha subunit 45kDa	−0.404	-1.541	−1.895
128232	PITPNM1	phosphatidylinositol transfer protein, membrane-associated 1	−0.454	-0.656	−1.644
111955	NR2F2	nuclear receptor subfamily 2, group F, member 2	−0.540	-0.758	−1.513
122343	FABP5	fatty acid binding protein 5 (psoriasis-associated)	−0.096	-0.703	−1.459
114356	ACSL3	acyl-CoA synthetase long-chain family member 3	−1.106	-1.981	−1.271
137968	OCRL	oculocerebrorenal syndrome of Lowe	0.022	-1.121	−0.937
102218	ACLY	ATP citrate lyase	−0.452	-1.418	−0.794
128174	CLU	clusterin	−0.089	-0.893	−0.747
128869	TMEM23	transmembrane protein 23	-0.967	-1.224	−0.420
171037	ALDH3A2	aldehyde dehydrogenase 3 family, member A2	-0.119	-1.163	−0.414
146593	ACADVL	acyl-Coenzyme A dehydrogenase, very long chain	0.733	0.820	−0.036
133876	ACOT7	acyl-CoA thioesterase 7	0.827	1.025	0.011
199757	CAV1	caveolin 1, caveolae protein, 22kDa	0.353	-0.485	−1.061
170041	NPC1	Niemann-Pick disease, type C1	−0.052	-0.583	−0.446
168754	OSBPL1A	oxysterol binding protein-like 1A	−0.642	−0.998	0.255
170102	PMVK	phosphomevalonate kinase	0.859	1.098	0.269
119370	PNPLA4	patatin-like phospholipase domain containing 4	0.792	0.843	0.403
112773	PCYT1A	phosphate cytidylyltransferase 1, choline, alpha	0.528	0.959	1.090
219614	SAMD8	sterile alpha motif domain containing 8	1.458	1.608	1.277
126373	STARD4	START domain containing 4, sterol regulated	−0.066	−0.332	1.347
145487	GPAM	glycerol-3-phosphate acyltransferase, mitochondrial	1.061	1.275	1.568
231296	PCSK9	proprotein convertase subtilisin/kexin type 9	0.392	0.313	1.765
161340	PAFAH1B2	platelet-activating factor acetylhydrolase, isoform Ib, beta subunit 30kDa	1.380	2.608	1.990
209566	IDI1	isopentenyl-diphosphate delta isomerase 1	−0.698	−0.951	1.651
154827	FDFT1	farnesyl-diphosphate farnesyltransferase 1	−0.129	−0.266	1.399
174731	HMGCR	3-hydroxy-3-methylglutaryl-CoenzymeA reductase	−0.248	0.201	2.073
193122	HMGCS1	3-hydroxy-3-methylglutaryl-Coenzyme A synthase 1 (soluble)	−0.082	1.00	2.820

Table 4. Stress-related genes regulated by EGCG

Probe id	Gene symbol	Gene name	6h ratio -log2	12h ratio -log2	24h ratio -log2
Transcription factors					
185687	ATF3	activating transcription factor 3	2.645	4.101	2.504
183867	ATF4	activating transcription factor 4	0.801	0.959	0.835
100596	CEBPG	CCAAT/enhancer binding protein (C/EBP), gamma	1.603	2.299	1.792
194114	FOXO3A	forkhead box O3A	1.092	1.695	1.038
Cell redox homeostasis/oxidative stress					
140616	DUSP23	dual specificity phosphatase 23	0.982	1.245	0.550
121612	DUSP5	dual specificity phosphatase 5	2.526	1.996	0.794
161352	DUSP3	dual specificity phosphatase 3 (vaccinia virus phosphatase VH1-related)	0.244	1.611	1.166
196828	GCLC	glutamate-cysteine ligase, catalytic subunit	0.388	0.370	1.032
196828	PRDX5	peroxiredoxin 5	0.494	0.728	1.034
149133	SOD2	Superoxide dismutase 2, mitochondrial	0.939	1.383	1.315
226167	TXNDC10	thioredoxin domain containing 10	0.541	1.117	1.528
179796	TXN2	thioredoxin 2	0.125	1.274	0.720
197013	SDF2L1	stromal cell-derived factor 2-like 1	1.098	1.694	0.846
DNA damage stimulus					
144049	BTG1	B-cell translocation gene 1, anti-proliferative	0.717	1.875	2.370
192182	RAD1	RAD1 homolog (S. pombe)	−0.109	0.568	1.232
234387	RAD23B	RAD23 homolog B (S. cerevisiae)	−0.296	−1.267	−1.587
184090	RAD18	RAD18 homolog (S. cerevisiae)	−0.044	−0.644	0.319
Cell cycle/apoptosis					
179446	BNIP2	BCL2/adenovirus E1B 19kDa interacting protein 2	0.617	1.222	1.106
109165	BNIP3	BCL2/adenovirus E1B 19kDa interacting protein 3	0.205	1.045	2.112
144168	BNIP3L	BCL2/adenovirus E1B 19kDa interacting protein 3-like	0.900	1.498	2.152
114136	CASP7	caspase 7, apoptosis-related cysteine peptidase	0.286	0.453	0.806
235779	CDK6	cyclin-dependent kinase 6	−0.698	−1.874	−2.044
207914	CCNJ	cyclin J	−0.685	−1.671	−1.456
207292	CCNT2	cyclin T2	−1.274	−1.851	−1.330
204006	CDKN2B	cyclin-dependent kinase inhibitor 2B (p15, inhibits CDK4)	1.391	1.147	0.910
137292	CDKN1A	cyclin-dependent kinase inhibitor 1A (p21, Cip1)	1.707	2.005	1.254
175225	NFKBIE	nuclear factor of kappa light polypeptide gene enhancer in B-cells inhibitor, epsilon	1.402	1.167	0.238
107316	PTEN	phosphatase and tensin homolog	−0.120	−0.184	0.898

EGCG increases expression of cellular stress and ER stress markers

Treatment with EGCG resulted in elevated expression of cellular stress markers, such as transcription factors, markers of DNA damage, cell cycle/apoptosis, and genes associated with redox status (Table 4). Of particular note, 3 genes-activating transcription factor 3 (ATF3), activating transcription factor 4 (ATF4), and CCAAT/enhancer binding protein (C/EBP), gamma (CEBPG)-are known to be associated with ER stress. The involvement of ER stress in EGCG-induced cytotoxicity was further monitored by real-time RT-PCR of differentially expressed marker genes (Fig. 3). The results showed that ATF3, which is a member of the ATF/CREB subfamily of the basic region leucine zipper (bZIP) family, was increased by more than 8-fold in 6-h-treated cells. In addition, members of the CCAAT/enhancer binding protein (C/EBP) family of transcription factors, such as the apoptosis-inducing proteins GADD153 (CHOP) and GADD34, were also upregulated in 6-h-treated cells. The expression of GADD153 and GADD34 was increased more than 2-fold at all time points.

Prolonged ER stress can perturb mitochondria, triggering oxidative stress. Ca^{2+}-induced oxidative stress can cause both cell death and activation of NF-κB signaling (Ji and Kaplowitz, 2006). In this study, NFKBIE was differentially expressed at 6 h (2.6-fold) and 12 h (2.2-fold), but at 24 h it was not significantly expressed (1.1-fold). NFKBIE is known as a member of the family of NF-κB inhibitory proteins (IκBs) that interact with NF-κB in unstimulated cells (Komissarova *et al*., 2008),

Verification of microarray data

To verify the gene expression profiles from the oligonucleotide microarray, 6 genes that showed significant up-

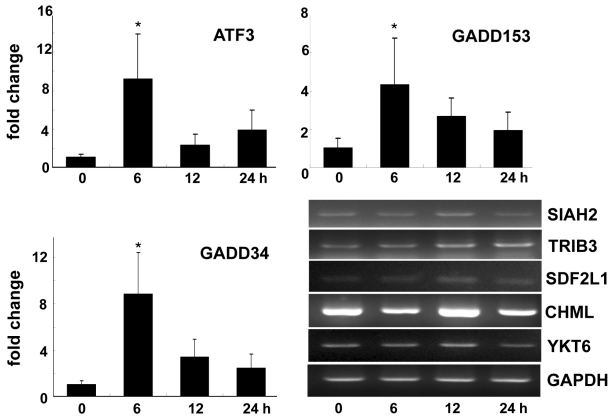

Fig. 3. Time sequences of gene expression, assayed by real-time and semiquantitative RT-PCR. Real-time PCR analysis was performed for GADD153, GADD43, and ATF3. Each value is expressed as the fold-change in mRNA levels at each time point and represents the mean±SEM of 3 independent experiments. Semiquantitative RT-PCR was also performed to verify the relative mRNA levels of randomly selected genes.

regulation were selected and subjected to semiquantitative RT-PCR analysis. The expression pattern observed by PCR showed a concordance with the pattern assayed by microarray (Fig. 3).

Discussion

The objective of this study was to determine the effects of EGCG on hepatic gene expression and to understand the underlying mechanism of hepatotoxicity for this polyphenol in vitro. Our study revealed that high concentrations of EGCG affected the expression of a large number of genes in various cellular pathways (1343 genes). The functional enrichment analysis of the differentially expressed genes provided new insight into the molecular mechanism of EGCG for its undesirable effect.

We showed that high concentrations of EGCG activate the unfolded protein response (UPR), resulting in increased expression of ER stress response genes in cultured human HepG2 cells. ER not only is the place of protein synthesis and package; it also plays a central role in various signaling pathways. Dysfunction of the ER can be induced by various biological disturbances, so-called ER stress. UPR is one of the well-known ER stresses, and it may be associated with cellular apoptosis in HepG2 cells. The UPR is reported to be required for safe-guarding protein synthesis, post-translational modifications, folding and secretion, calcium storage, and calcium signaling in the normal physiological state.

In our study, EGCG exposure to HepG2 cell cultures resulted in a marked increase in the mRNA level of genes associated with protein synthesis and modification. This is not surprising, because repairing hepatic damage requires the massive production of new proteins and modification of proteins. EGCG treatment also revealed upregulation of many genes involved in protein secretion, including intracellular protein trafficking. These expression patterns were consistent with those of pyrazole, a known inducer of ER stress (Nichols and Kirby, 2008).

EGCG-induced upregulation of GADD34, GADD153, and ATF3 provides genetic evidence for the presence of EGCG-caused ER stress. Even though GADD153, a member of the C/EBP gene family of transcription factors, has already been reported to be induced by growth arrest, DNA damage, or UV irradiation, recent studies have demonstrated that the gene also has great responsivity to ER stress (Outinen *et al*., 1999; Wang *et al*., 1996). In addition, it has previously been shown that GADD153 induces cell death by promoting protein synthesis and oxidation in the stressed endoplasmic reticulum (Marciniak *et al*., 2004). The transcription of ATF3 usually increases within 2 h from stress exposure, and ATF3 protein can function as a homodimer or as a member of the complex of the CCAAT/enhancer binding protein (C/EBP) family of transcription factor, such as GADD153. Jiang *et al*. (2003) also found that ATF3 is induced in response to ER stress. GADD34 encodes a regulatory subunit of an eIF2α-directed-phosphatase complex that promotes the recovery of protein synthesis in cells exposed to ER stress, causing more ER stress (Lai *et al*., 2007).

In addition to genes related to ER stress, apoptosis-related genes, like BNIP3 and BNIP3L, were also upregulated around 2-fold after 12 h and around 4-fold after 24 h of EGCG treatment in HepG2 cells. According to a previous report, induction of BNIP3 localized itself to mitochondria and triggered a loss of membrane potential and an increase in reactive oxygen species production, which often lead to cell death (Burton and Gibson, 2009). These results imply that EGCG exposure to HepG2 cells induces BNIP-mediated apoptosis through disturbances of ER functions.

There have been various studies to elucidate the molecular mechanism of EGCG activity. Although some EGCG-interacting molecules have been identified, the molecular mechanism of its cytotoxic activity is not yet fully clarified. Recently, Kuzuhara *et al*. (2006) reported that EGCG and its related derivatives that have a galloyl group interacted with DNA and RNA directly, while catechin and its related derivatives, lacking a galloyl group,

did not interact with DNA or RNA. On the other hand, Ermakova *et al*. (2006) reported that glucose-regulating protein 78 (GRP78), a molecular chaperone in the ER, is an EGCG-binding protein. In the report, EGCG and catechins, containing a galloyl group, showed stronger inhibition of GRP78 than EC, EGC, and catechins that lacked a galloyl group. This observation strongly supports the existence of an interaction between the galloyl group and GRP78.

ER stress contributes to intracellular lipid accumulation, which is mediated by ER-associated transmembrane sterol response element-binding protein 1 (SREBP1), an ER membrane-bound transcription factor. SREBP1 activates genes encoding enzymes in the cholesterol/triglyceride biosynthesis and uptake pathway (Ji and Kaplowitz, 2006). The present study showed that EGCG-induced ER stress increased the expression of genes responsible for cholesterol/triglyceride biosynthesis, including HMGCR and HMGCS1, and decreased the expression of genes responsible for lipid transport, including CAV1, NPC1, OSBPL1A, and CLU. Interestingly, clusterin (CLU), a multifunctional heterodimeric glycoprotein, is known for its implication in a wide range of physiological functions, such as lipid transport, tissue repair and remodeling, membrane protection, and promotion of cell interaction. It has been reported that induction of clusterin may represent a protective response against oxidative stress (Shannan *et al*., 2006). More recently, clusterin has been proposed as a candidate biomarker for kidney injury (Sieber *et al*., 2009).

Based on the analyses of the presented microarray data, it seems clear that high concentrations of EGCG cause cell death, probably via the apoptosis pathway, by inducing ER stress and the expression of ER stress response genes (GADD153, GADD34, and ATF3). The presented results strongly suggest that high concentrations of EGCG might cause fatty liver through ER stress-induced accumulation of lipids in living subjects. The identification of other regulatory genes may also aid in clarifying the molecular mechanism underlying EGCG-induced hepatotoxicity.

References

Burton, T.R., and Gibson, S.B. (2009). The role of Bcl-2 family member BNIP3 in cell death and disease: NIPping at the heels of cell death. *Cell Death Differ.* 16, 515-523.

Dodo, K., Minato, T., Noguchi-Yachide, T., Suganuma, M., and Hashimoto, Y. (2008). Antiproliferative and apoptosis-inducing activities of alkyl gallate and gallamide derivatives related to (-)-epigallocatechin gallate. *Bioorg. Med. Chem.* 16, 7975-7982.

Ermakova, S.P., Kang, B.S., Choi, B.Y., Choi, H.S., Schuster, T.F., Ma, W.Y., Bode, A.M., and Dong, Z. (2006). (-)-Epigallocatechin gallate overcomes resistance to etoposide-induced cell death by targeting the molecular chaperone glucose-regulated protein 78. *Cancer Res.* 66, 9260-9269.

Galati, G., Lin, A., Sultan, A.M., and O'Brien, P.J. (2006). Cellular and in vivo hepatotoxicity caused by green tea phenolic acids and catechins. *Free Radic. Biol. Med.* 40, 570-580.

Goodin, M.G., and Rosengren, R.J. (2003). Epigallocatechin gallate modulates CYP450 isoforms in the female Swiss-Webster mouse. *Toxicol. Sci.* 76, 262-270.

Isbrucker R.A., Edwards, J.A., Wolz, E., Davidovich, A., and Bausch, J. (2006). Safety studies on epigallocatechin gallate (EGCG) preparations. Part 3: teratogenicity and reproductive toxicity studies in rats. *Food Chem. Toxicol.* 44, 651-661.

Ji, C., and Kaplowitz, N. (2006). ER stress: can the liver cope? *J. Hepatol.* 45, 321-333.

Jiang, H.Y., Wek, S.A., McGrath, B.C., Lu, D., Hai, T., Harding, H.P., Wang, X., Ron, D., Cavener, D.R., and Wek, R.C. (2004). Activating transcription factor 3 is integral to the eukaryotic initiation factor 2 kinase stress response. *Mol. Cell. Biol.* 24, 1365-1377.

Komissarova, E.V., Li, P., Uddin, A.N., Chen, X., Nadas, A., and Rossman, T.G. (2008). Gene expression levels in normal human lymphoblasts with variable sensitivities to arsenite: identification of GGT1 and NFKBIE expression levels as possible biomarkers of susceptibility. *Toxicol. Appl. Pharmacol.* 226, 199-205.

Kuzuhara, T., Sei, Y., Yamaguchi, K., Suganuma, M., and Fujiki, H. (2006). DNA and RNA as new binding targets of green tea catechins. *J. Biol. Chem.* 281, 17446-17456.

Lai, E., Teodoro, T., and Volchuk, A. (2007). Endoplasmic reticulum stress: signaling the unfolded protein response. *Physiology* 22, 193-201.

Lambert, J.D., Sang, S., and Yang, C.S. (2007). Possible controversy over dietary polyphenols: benefits vs risks. *Chem. Res. Toxicol.* 20, 583-585.

Marciniak, S.J., Yun, C.Y., Oyadomari, S., Novoa, I., Zhang, Y., Jungreis, R., Nagata, K., Harding, H.P., and Ron, D. (2004). CHOP induces death by promoting protein synthesis and oxidation in the stressed endoplasmic reticulum. *Genes Dev.* 18, 3066-3077.

Nichols, K.D., and Kirby, G.M. (2008). Microarray analysis of hepatic gene expression in pyrazole-mediated hepatotoxicity: identification of potential stimuli of Cyp2a5 induction. *Biochem. Pharmacol.* 75, 538-551.

Outinen, P.A., Sood, S.K., Pfeifer, S.I., Pamidi, S., Podor, T.J., Li, J., Weitz, J.I., and Austin, R.C. (1999). Homocysteine-induced endoplasmic reticulum stress and growth arrest leads to specific changes in gene expression in human vascular endothelial cells. *Blood* 94, 959-967.

Pacheco, C.D., and Lieberman, A.P. (2008). The pathogenesis of Niemann-Pick type C disease: a role for autophagy? *Expert Rev. Mol. Med.* 10, e26.

Schmidt, M., Schmitz, H.J., Baumgart, A., Guédon, D., Netsch, M.I., Kreuter, M.H., Schmidlin, C.B., and Schrenk, D. (2005). Toxicity of green tea extracts and

their constituents in rat hepatocytes in primary culture. *Food Chem. Toxicol.* 43, 307-314.

Shannan, B., Seifert, M., Leskov, K., Willis, J., Boothman, D., Tilgen, W., and Reichrath, J. (2006). Challenge and promise: roles for clusterin in pathogenesis, progression and therapy of cancer. *Cell Death Differ.* 13, 12-19.

Sieber, M., Hoffmann, D., Adler, M., Vaidya, V.S., Clement, M., Bonventre, J.V., Zidek, N., Rached, E., Amberg, A., Callanan, J.J., Dekant, W., and Mally, A. (2009). Comparative analysis of novel noninvasive renal biomarkers and metabonomic changes in a rat model of gentamicin nephrotoxicity. *Toxicol. Sci.* 109, 336-349.

Vittal, R., Selvanayagam, Z.E., Sun, Y., Hong, J., Liu, F., Chin, K.V., and Yang, C.S. (2004). Gene expression changes induced by green tea polyphenol (-)-epigallocatechin-3-gallate in human bronchial epithelial 21BES cells analyzed by DNA microarray. *Mol. Cancer Ther.* 3, 1091-1099.

Wang, X.Z., Lawson, B., Brewer, J.W., Zinszner, H., Sanjay, A., Mi, L.J., Boorstein, R., Kreibich, G., Hendershot, L.M., and Ron, D. (1996). Signals from the stressed endoplasmic reticulum induce C/EBP-homologous protein (CHOP/GADD153). *Mol. Cell. Biol.* 16, 4273-4280.